

# Studies on polypyrrole film in room temperature melt

S. Geetha, D.C. Trivedi\*

*Electrochemical Materials Science Division, Centre for Conducting Polymers, Central Electrochemical Research Institute, Karaikudi 630 006, India*

Received 22 June 2004; received in revised form 26 July 2004; accepted 10 August 2004

## Abstract

A bluish-black shining free standing polypyrrole film (PPy) of electronic conductivity  $\sim 130 \text{ S cm}^{-1}$  has been prepared by electrochemical oxidative polymerization of pyrrole on Pt/transparent glass conducting electrode  $\sim$  resistance  $15 \Omega \text{ cm}^{-1}$ , using a room temperature melt as an electrolyte, composed of 1:3 stoichiometric ratio of cetyl pyridinium chloride and anhydrous aluminum chloride at 0.58 V versus Al wire as a reference electrode. The film possessed a charge transfer resistance of  $132 \Omega$ , and showed two absorption peaks at 457 and 1264 nm in the UV-vis–NIR diffused reflectance spectra. The morphology of the film was hexagonal. The potential step technique suggested a layered structure. This thin film can easily be peeled off from the electrode surface after three cycles and can be used for various applications like dissipation of electrostatic charge, battery electrode materials, solid electrolytic capacitor, electrochromic windows and displays, microactuators etc. It was also characterized by IR, thermal and SEM studies.

© 2004 Elsevier B.V. All rights reserved.

**Keywords:** Polypyrrole; Conductivity; Free standing; Room temperature melt; Cetyl pyridinium chloroaluminate melt

## 1. Introduction

In recent years, conducting polymers with conjugated double bonds have attracted much attention as advanced materials. Among these conducting polymers, polypyrrole (PPy) is a promising material for commercial applications because of its good environmental stability, easy electrochemical preparation and biocompatibility.

Pyrrole is susceptible to aerial oxidation and gets readily polymerized to give a black conducting powder [1]. This chemistry is particularly taking place on the outside of the bottles of pyrrole down which the monomer has been allowed to flow. The resulting conducting powder have been referred to as pyrrole black for many years. Oxidation of these powders with  $\text{KMnO}_4$  has been shown to lead predominantly 2,5 dicarboxylic acid and this has been interpreted as evidence that the polymerization leads to an  $\alpha$ - $\alpha'$  bonded polymer [1]. The polymerization can take place chemically and

electrochemically [2]. Chemically pyrrole can be oxidatively polymerized in both solution and vapor phase [3]. Though chemical oxidation usually leads to powders, films can be obtained by allowing the oxidation to take place at a solid or liquid surface [3,4], however these films are of poor quality. Thus, eventhough preparation of polypyrrole films remains a desirable goal, presently the electrochemical synthesis provides the only satisfactory route. Good quality films were first obtained by Kanazawa et al [5,6] and Diaz et al [7], using modification of the electrochemical technique, pioneered by Dall'aglio et al. [2].

PPy can often be used as biosensors [8,9], gas sensors [10,11], wires [12], microactuators [13], antielectrostatic coatings [14], solid electrolytic capacitor [15,16], electrochromic windows and displays, and packaging, polymeric batteries, electronic devices and functional membranes, etc. [17–19]. PPy coatings have an excellent thermal stability and are good candidate for use in carbon composites [20]. Furthermore, the electrochemical process parameters affecting the properties of the PPy coatings are also investigated [21]. However, synthetically conductive PPy is insoluble and infusible, which restricts its processing and applications in other fields. The problem has been extensively investigated

\* Corresponding author. Tel.: +91-456-522-7775; fax: +91-456-522-7713.

E-mail addresses: [trivedi\\_dc@rediffmail.com](mailto:trivedi_dc@rediffmail.com), [trivedi@cecri.res.in](mailto:trivedi@cecri.res.in) (D.C. Trivedi).

and new application fields have also been explored in the past several years. For example, PPy-based polymers can be used to load and release drugs and biomolecules [22]. PPy-based polymer blends can protect the corrosion of metals [23]. Because of the strong adhesion of PPy to iron or steel treated with nitric acid, PPy polymers can be used as good adhesives [24]. In a recent report [25], PPy-modified tips for functional group recognition are applied in scanning tunneling microscopy. Here, we are introducing a novel method to synthesize highly conducting polypyrrole film, using chloroaluminate room temperature melt as the electrolyte.

## 2. Experimental

### 2.1. Reagents

Anhydrous aluminum chloride, recrystallized cetyl pyridinium chloride and distilled pyrrole were used (Sigma-Aldrich.).

### 2.2. Preparation of electrolyte

Cetyl pyridinium chloride (67%) and aluminum chloride (33%) were mixed together thoroughly inside a dry box to get a highly viscous liquid (melt). The proportion of aluminum chloride is always maintained to be higher than cetyl pyridinium chloride to get the acidic melt. This viscous melt is dissolved in diethylether (solvent) to reduce the viscosity.

### 2.3. Electrochemical polymerization

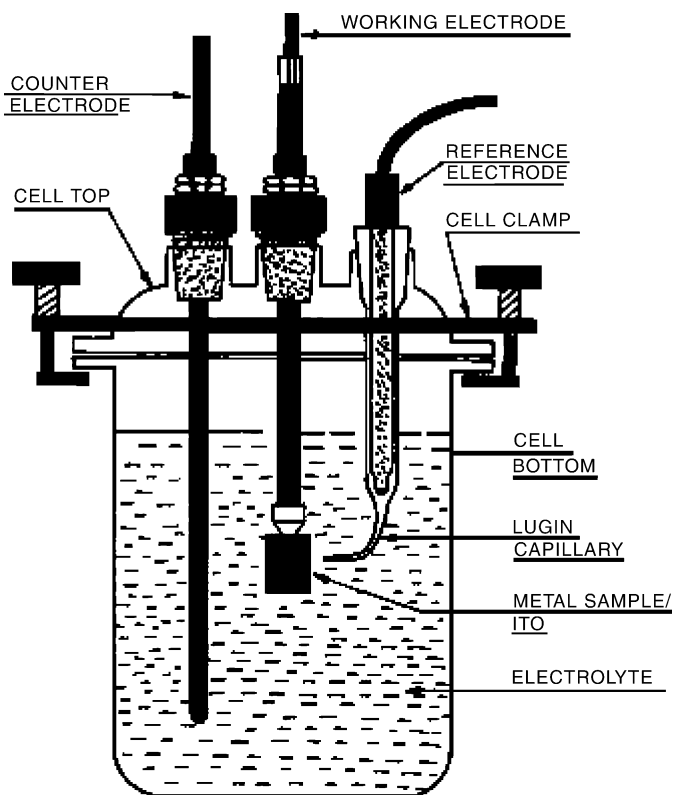
The electro polymerization of pyrrole was carried out by potentiodynamic technique, using EG & G PARC Model175 universal programmer and Tacussel bi-pad type potentiostat with BBC-GOERZ METRAWATT SE790 model recorder at room temperature. A three compartment sealed glass electrochemical cell was used with platinum sheet as the working electrode and platinum wire was used as the counter electrode. A high purity aluminum wire was used as the reference electrode. The electrochemical cell type used in the process is shown in Scheme 1. The electro deposition of PPy was carried out by sweeping potential at  $50 \text{ mV s}^{-1}$  in the potential range of 0 and 1.1 V versus Al wire from the 0.1 M electrolyte prepared by adding the room temperature melt in pyrrole.

### 2.4. Characterization

The characterization of PPy film was carried out under anhydrous conditions by electrochemical techniques, spectroscopic methods, conductivity measurements, thermal analysis and scanning electron micrograph.

#### 2.4.1. Electrochemical characterization

The electrochemical characterization was carried out by cyclic voltammetric experiments at various sweep rates, elec-



Scheme 1. General set-up for electrochemical polymerization.

trochemical impedance studies and electrochemical growth by step potential techniques.

**2.4.1.1. Cyclic voltammetric studies.** The electrochemical characterization was done by potentiodynamic technique, using EG & G PARC Model175 universal programmer and Tacussel bi-pad type potentiostat with BBC-GOERZ METRAWATT SE790 model recorder at room temperature.

**2.4.1.2. Impedance studies.** The impedance studies were carried out, using EG & G impedance analyzer (Princeton Applied Research, USA model no.6310) under open circuit potential in the ac frequency range 100 kHz to 0.1 Hz with an amplitude of the excitation signal of 10 mV.

**2.4.1.3. Electrochemical growth—potential step technique.** The growth of the polymer film was studied at various potentials by potential step technique, using EG & G PARC Model175 universal programmer and Tacussel bi-pad type potentiostat with BBC-GOERZ METRAWATT SE790 model recorder. All studies were carried out at room temperature.

#### 2.4.2. Conductivity measurements

The electronic conductivity measurements were carried out by four probe method, using Keithley Model 2400 series Source meter and Keithley Model 2182 Nano voltmeter equipment under nitrogen atmosphere.

### 2.4.3. Electronic spectral studies

UV spectra of the electrode surface were recorded on Cary 500 scan UV–vis–NIR spectrophotometer, using high alumina pellet as reference in the range 200–1500 nm.

### 2.4.4. Vibrational spectral studies

FTIR spectra were recorded, using Perkin–Elmer Paragon–500 FTIR spectrophotometer, using KBr pellets in the region between 400 and 4000  $\text{cm}^{-1}$ .

### 2.4.5. Thermal analysis

The thermal studies were carried out in the air at the heating rate of  $10^\circ \text{min}^{-1}$ , using Simultaneous Thermal Analyzer (Model No STA 1500, PL Thermal Sciences, UK).

### 2.4.6. Morphology—scanning electron micrograph

Scanning electron micrographs were recorded at various magnifications, using Hitachi-S-3000H SEM machine.

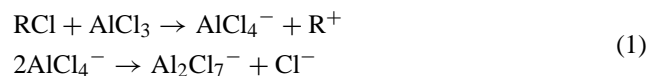
## 3. Results and discussions

### 3.1. Film appearance

The color of the PPy film depends on the thickness and varies from dark green to black in doped state on the platinum substrate. The film turned to blue in the undoped state which was obtained by washing with aqueous ammonia and final washings with water for 4 h.

### 3.2. Innovation of the melt

Interest in room temperature melt in the study of conducting polymers is due to the fact that electrolyte is free from solvent, thus one can prevent a side reaction of a solvent molecule with moderately stable radical cation generated during electrochemical synthesis near the vicinity of an anode. Thus, the electrolyte devoid of solvent can yield a better-oriented polymer with better conjugation and electronic conductivity. However, these melts in the synthesis of conducting polymers were elusive, because of the cathodic deposition of aluminum, thereby, non-availability of  $\text{AlCl}_4^-/\text{Al}_2\text{Cl}_7^-$  to initiate the polymerization reaction in an electrochemical version of Friedel Crafts reaction and also to act as a dopant. Trivedi [26] carried out extensive work on this aspect and found that when bulky cetyl pyridinium chloride is used to prepare a room temperature melt, the cathodic deposition of aluminum is completely inhibited due to preferential absorption of bulky cetyl groups on the cathode. The other chloroaluminate melts are vogue to study the generation of organic cations due to its wide electrochemical window, which is extended upto 4.4 V.



This melt has been found to be useful as an electrolyte in battery systems, using conducting polymers. Acidic ionic liquids with chloroaluminate ions proved to be effective Friedel Crafts catalysts [27].

### 3.2.1. CV studies—electrochemical polymerization of pyrrole by cyclic voltammetry

The growth of conducting polymer film has been a subject of intensive studies by various techniques to understand its various properties like ion transport and optical studies. In principle, the growth of the conducting polymer can be compared with electrodeposition of metals, the difference being that the former is an anodic reaction. The filming on an anode surface during electrolysis of a monomer in a suitable electrolytic medium occurs via oxidative generation of radical cations near the vicinity of an anode which on further coupling leads to precipitation of conducting polymer leading to a filming anode surface suggesting that particles are added one at a time to a cluster or aggregate of particles via random walk trajectories, that is to say that competing growth of polymer on anode surface leads to formation of a cluster and can be considered as an alloy of macromolecule with counter ion giving it a distinct entity.

The electrodeposition reaction from solution phase is a transformation reaction, thus there is a tendency in the system between order and disorder, which results in thermodynamic fluctuations leading to the formation of an ordered phase.

The electrochemical polymerization of pyrrole to free-standing polypyrrole (PPy) film in room temperature melt is shown in Fig. 1. The growth is reflected by the increase

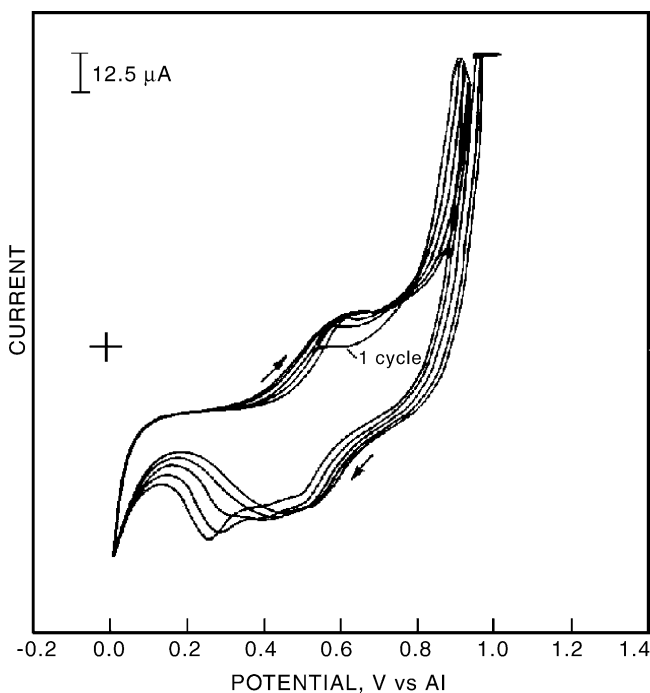


Fig. 1. Electrochemical growth pattern of polypyrrole in the presence of chloroaluminate room temperature melt as the electrolyte, potential range  $-0.2$  to  $1.2$  V vs. Al at sweep rate of  $50 \text{ mV s}^{-1}$ .

in peak current. The color of the film was black. The electropolymerization of pyrrole to freestanding polypyrrole film in chloroaluminate room temperature melt medium was carried out by potentiodynamic method. In the very first cycle of polymerization the peak appearing at 0.5 V corresponds to the oxidation of pyrrole to pyrrole radical cation. In subsequent cycles, new oxidation peaks appear at 0.58 V indicating that these radical cations undergo further coupling and the peak current increases continuously with successive potential scans indicating the buildup of electroactive polypyrrole on the electrode surface. Though the peak potential of the peak observed in the first cycle is at 0.5 V (very broad: formation beginning around at 0.45 V), this suggests that even by keeping the potential around this value can lead to formation of polymer at a slow growth rate, which is beneficial for obtaining a more ordered thin polymer film useful for electrochromic displays. Once the polymerization process is initiated it is influenced by the anion for the following factors:

- Adsorption of the anion on the electrode surface;
- Redox potential of the anion;
- The ionic charge;
- The ionic size and
- The hydration shell.

Electrochemical studies reveal the influence of the counter anion on the peak potentials as well as on the polymer deposition rate indicating that the electron transfer and protonation processes are greatly influenced by the anion.

The electro active PPy is obtained only when the melt is acidic, i.e. the proportion of aluminum chloride in the melt is more giving rise to  $\text{AlCl}_4^-$  anion, which is the dopant responsible for the oxidation of pyrrole. The electro polymerization does not occur in the neutral or basic melts.

In the forward cycle, during growth a well-defined peak was observed at 0.58 V versus Al wire which is shifted to 0.6 V with increase in scan numbers and similarly in the reverse cycle two peaks were observed at 0.56 V which is shifted slightly to 0.55 V and at 0.4 V versus Al wire which is shifted to 0.2 V in the negative side. This shows that the polymerization reaction is reversible.

Fig. 2 shows the cyclic voltammogram for PPy on Pt electrode surface ( $0.25 \text{ cm}^2$ ) in 1 M chloroaluminate room temperature melt electrolyte diluted in diethyl ether (without the monomer) at the scan rate of  $50 \text{ mV s}^{-1}$ . It shows a significant redox peak at 0.85 V and at 1.1 V in the forward cycle and at 0.38 V in the reverse cycle. In order to explain the electrochemical behavior of PPy, the radical cations are oxidized to give PPy in observed loop. The doping and dedoping mechanism corresponding to different potentials is given in Scheme 2.

The decrease in polymerization potential in a solvent free medium is probably due to the fact that all nucleophilic secondary reactions are inhibited. The adhesion of the polymer film to the electrode surface was also observed which is in good agreement with the Fowkes theory [28]. The adsorption

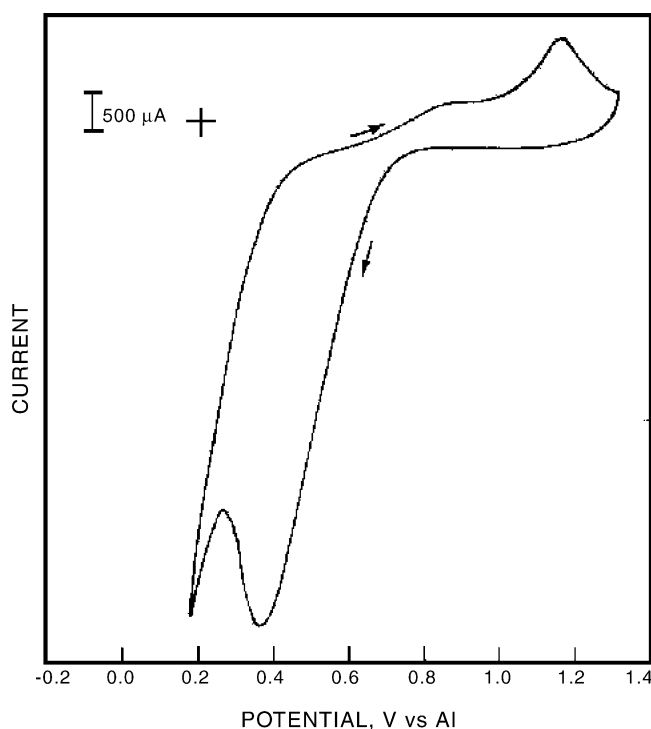
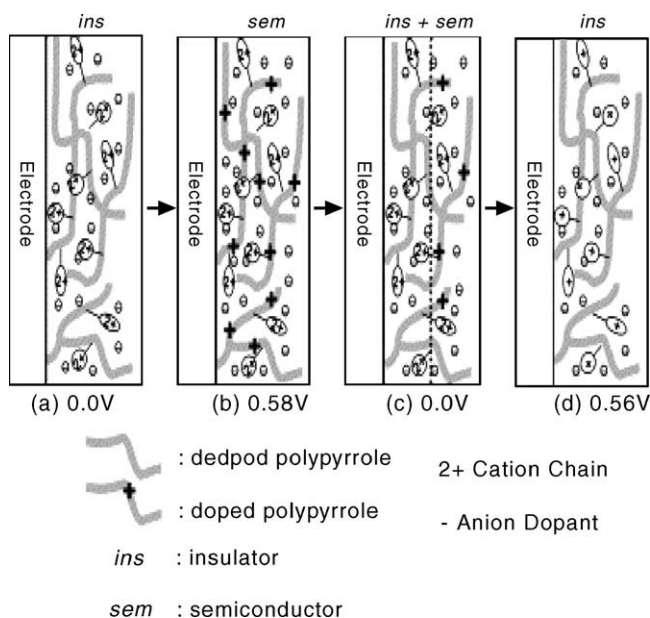


Fig. 2. Cyclic voltammogram of polypyrrole in the absence of monomer, potential range 0 to 1.2 V vs. Al at a sweep rate of  $50 \text{ mV s}^{-1}$ .

of the polymer from the organic solvents onto inorganic surfaces is a process involving acid–base interactions between polymer and solvent and between solid and solid, a triangular competition.



Scheme 2. Doping and dedoping mechanism of polypyrrole at various potentials in cyclic voltametry.

### 3.3. Electrochemical properties

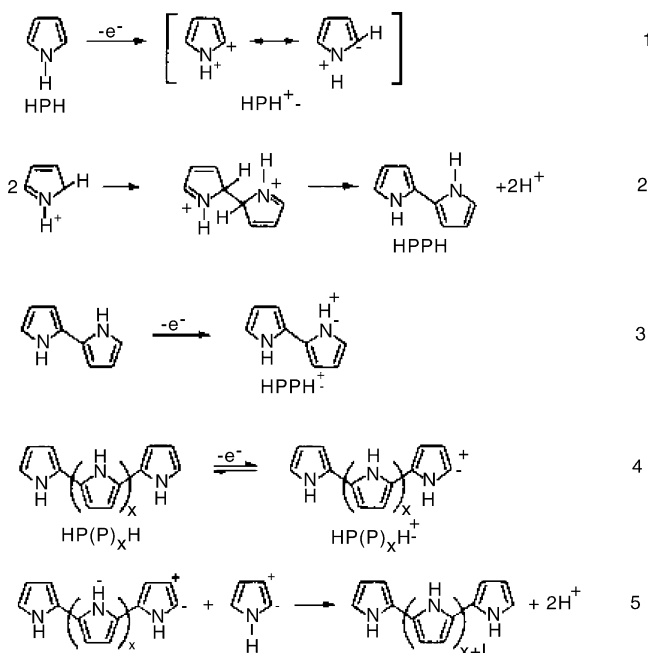
The electrochemistry of various pyrrole monomers and polymers has been studied extensively by Diaz and Kanazawa [29] Bidan and others [30]. Although, the polymer is prepared in its oxidized conducting state by a simultaneous polymerization and oxidation of the  $\pi$  system of the resulting polymer, the films can be reduced electrochemically or chemically to the neutral polymer. The neutral polymer has played a vital role in the characterization of the pyrrole system [3]. Hence, pyrrole was undoped by dissolving in ammonia solution or in sodium hydroxide solution for 1 h, washing with distilled water and then drying. The electrochemical switching between the conducting and insulating state is accompanied by a color change and could form the basis of the electrochromic display [29]. The electrochemical mechanism is given in Scheme 3.

In the given reaction Scheme 3, the initial oxidation reduction of the monomer gives a radical cation  $\text{HPH}^+$  that couples to form the dimer with expulsion of  $2\text{H}^+$ . This process is repeated with  $2e^-$  and  $2\text{H}^+$  involved in each addition step. The oxidation potential of the polymer is always lower than that of the monomer, and, thus reaction 5 is always favoured.

The final monomer is in the oxidized form and is generally associated with one anion per 3–4 monomer unit.

### 3.4. Potential step technique—nucleation studies

The potential step technique has been used to investigate nucleation and growth of PPy. In this experiment, a sudden higher potential is applied to the working electrode and the current and time transients are recorded. The shape of the transient indicates how the nucleation for the growth of poly-



Scheme 3. Mechanism for electropolymerization of pyrrole.

mer takes place. The nucleation gets influenced by following factors:

- (i) Nature of anion present;
- (ii) Concentration of the monomer and
- (iii) Preparation of the electrode surface.

After each experiment, the electrode surface has to be cleaned and reconditioned. The polymer growth was studied by fixing potential and time scale. The experimental set up was the same as that for CV studies. The growth of the conducting polymer can be compared with the electrodeposition of metals, the difference being that the former is an anodic reaction. In 1981, the diffusion limited aggregation (DLA) model was introduced by Witten and Sanders [31]. In this model, particles are added one at a time, to a cluster or aggregate of particles via random walk trajectories. According to this model, there is competing growth of polymer chains from a surface, which leads to the formation of independent clusters. Meakin [32] modified the DLA model, in which the growth process is in a direction perpendicular to the surfaces of growth sites. Initially, each site at the electrode surface is active. Random walkers (radicals) are launched one at a time and eventually either move a long distance from the growing deposit and are terminated or find an active site. If an active site is found this site becomes inactive and the site occupied by the random walker before it enters the active sites become the new active site. That is, how the surface of an electrode becomes covered progressively. Electrodeposition of conducting polymers is a polynucleation process and transients are triggered by single potential step. Nucleation is independent of the size and shape of the electrode and polynucleation starts in synchronism with the potential step and is illustrated in Fig. 3. The current-time transient can be replotted, using various equations as given by Li and Albery [33]. Fig. 3 shows the potential step growth of PPy at 0.6 V versus Al wire, as per CV curve Fig. 1 the growth of the polymer occurs at 0.58 V and at 0.6 V the CV curve has the

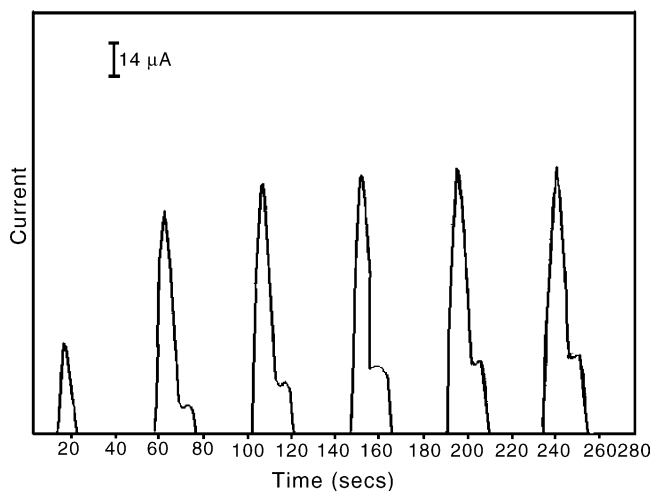


Fig. 3. Current vs. time response of a polypyrrole growth in the presence of room temperature melt at 0.6 V vs. Al wire for 10 s.



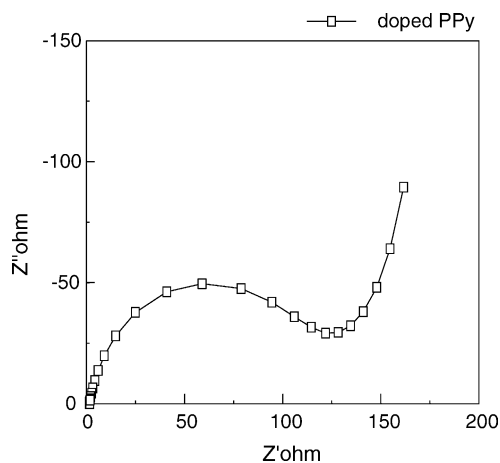


Fig. 4. Impedance spectra of doped PPy film in the ac frequency range 100 kHz–0.1 Hz with an excitation signal of 10 mV.

maximum current. To observe proper growth transients, time scale was fixed at  $10 \text{ s cm}^{-1}$  with a total growth time of 280 s. There is rise in the current from 166 to 229  $\mu\text{A}$  in steps. The steps in the growth curve, indicates the formation of a layered structure, which is uncommon in conducting polymers. The growth processes depend upon the following factors:

- i) Monomer concentrations;
- ii) Oligomerizations;
- iii) Diffusion of monomer into polymer film and
- iv) Formation of critical cluster and nucleus.

In CV curve, the random adsorption of monomer on a bare-electrode surface is seen more clearly in a deposition curve where relatively a broad peak appears at potentials significantly less positive than required for bulk oxidation of monomer and is followed by sharp peaks resulting from nucleation and monolayer spreading. The sharp rising edge of these peaks is linear with time, which suggests that two-dimensional patch has been expanding in a shape preserving

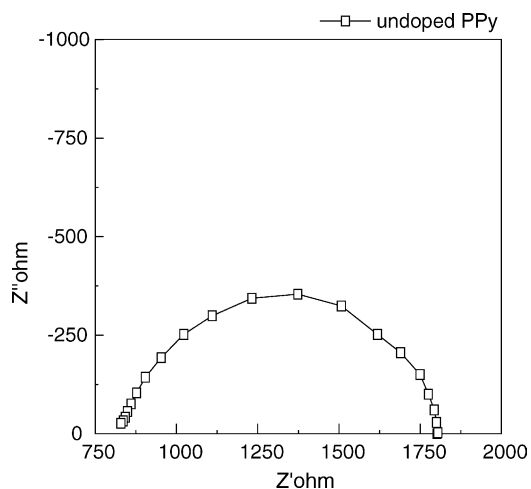


Fig. 5. Impedance spectra of undoped PPy film in the ac frequency range 100 kHz–0.1 Hz with an excitation signal of 10 mV.

Table 1  
Rs, Rct and C values of doped and undoped PPy film from complex plane impedance spectra (Figs. 4 and 5)

Nature of polymer film	Rs ( $\Omega$ )	Rct ( $\Omega$ )	C (Farads)
Doped PPy	1.0495	132.27	$8.8505 \times 10^{-5}$
Undoped PPy	824.89	1001.49	$2.00659 \times 10^{-6}$

Rs: solution resistance; Rct: charge transfer resistance; C: capacitance.

way. The close similarity of the peaks shape suggests that nucleation has occurred repeatedly on the same site.

### 3.5. Impedance studies

The impedance spectra of conducting polymer matrix deposited, using constant polarization mode may be considered to study the characteristics of film structures and the charge transfer resistance and ion transport in the metal/polymer interface and polymer film/electrolyte interface. After preparation of PPy film by constant polarization mode the film was subjected to an ac field under open circuit potential in the frequency range 100 kHz–0.1 Hz with an amplitude of the excitation signal of 10 mV. Figs. 4 and 5 gives the impedance spectra of doped and virgin PPy films in the room temperature melt.

As can be seen in figures of doped and undoped, the doping process dramatically modifies the impedance response of the systems. The semicircle obtained from the high-frequency region is ascribed to the blocking properties of a single electrode, which render extremely slow the faradic process of the ion-exchange at the polymer/electrolyte interface [34].

The electrochemical impedance for undoped PPy shows semicircle only in the high frequency region and there is no

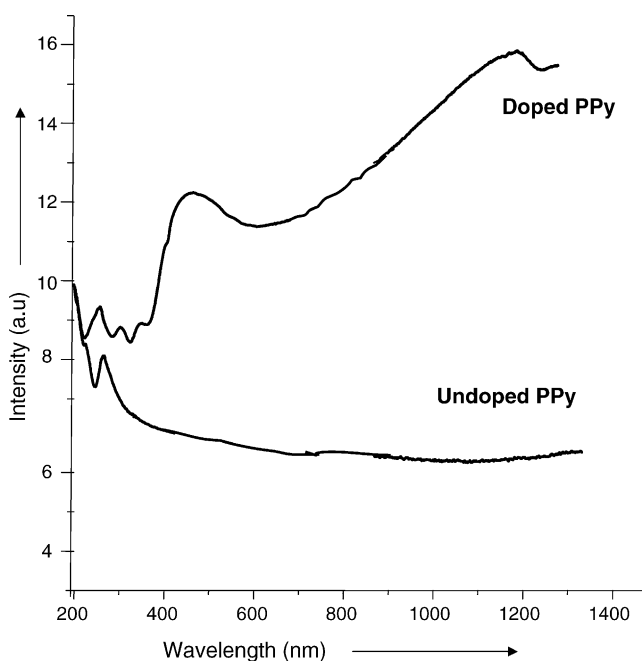


Fig. 6. The diffused reflectance UV spectra of (a) doped and (b) undoped PPy, using high alumina as reference in the range 200–1500 nm.

Table 2  
The major shifts of bands in FTIR spectra of doped PPy from virgin PPP (Fig. 7)

Assignment of IR bands	Undoped PPy	Doped PPy
	3421 $\text{cm}^{-1}$ (NH str)	No band
	3100 $\text{cm}^{-1}$ (C–H str)	Diminished band
	1535 $\text{cm}^{-1}$ (C=C and C–C str)	1529 $\text{cm}^{-1}$
	1450 $\text{cm}^{-1}$ (N–H str)	1445 $\text{cm}^{-1}$
	1295 $\text{cm}^{-1}$ (C–H and N–H def)	1290 $\text{cm}^{-1}$
	1050 $\text{cm}^{-1}$ (C–H def)	1010 $\text{cm}^{-1}$

diffusion impedance in the low frequency region. It reveals that the system is controlled by activation, whereas the EIS of the doped PPy shows a semicircle in the high frequency region and a straight line with slope of nearly  $45^\circ$  in the low frequency region, Warburg diffusion impedance. The high value at the low frequency side may be due to diffusional impedance created by the charge carriers across the polymer/electrode/electrolyte interface and this is bound to be higher and this is understandable from the low capacitance value  $8.8 \mu\text{F}$ . This may be due to the diffusion of  $\text{AlCl}_4^-$  dopant ion across the interface and consequently to the decrease in the mobility of the dopant ions. Regarding the semicircles, both in doped (uncompleted) and in undoped (completed) forms are somehow compressed indicating a relaxation process. When a 'Nyquist plot contains a depressed semicircle with the center at the real axis' such behavior is characteristic for solid electrodes and often referred to as frequency dispersion and has been attributed to roughness and other inhomogeneties of the solid surface. [35,36]. Nor-

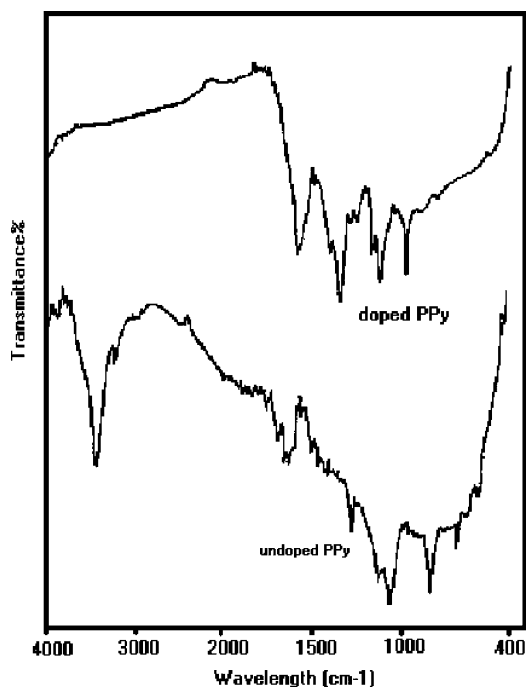


Fig. 7. FTIR spectra of doped (a) and undoped PPy (b) in the region  $4000 \text{ cm}^{-1}$  to  $400 \text{ cm}^{-1}$  in the KBr medium.

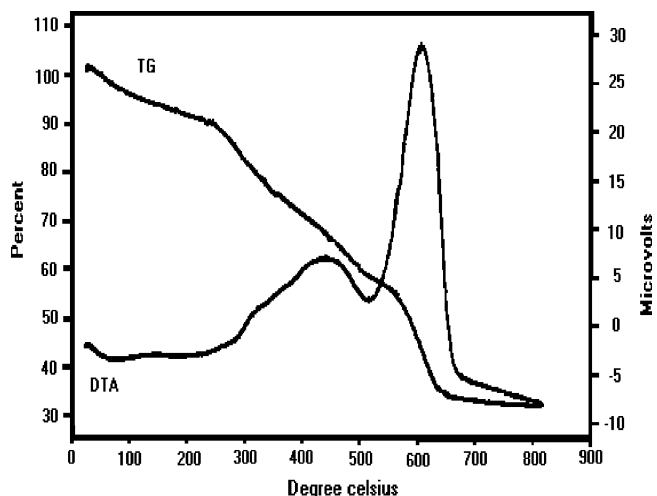


Fig. 8. TG/DTA curve for doped PPy.

mally, the intercept of Warburg impedance (corresponding to  $Z''$  minimum) should lead to a value of dc conductivity. From the impedance plot, this value seems to be  $132 \Omega$  for the doped species and this value will not correspond with the measured dc conductivity. This is because, the semicircle corresponds to various processes taking place at the electrode/electrolyte interface. The method of finding the dc conductivity by extrapolating the low frequency Warburg behavior will be valid only for simple cases, and, hence this method of getting dc conductivity value is not appropriate in the present case. In spite of similar shape of impedance spectra, there is a remarkable difference in the diameters of the two semicircles, i.e. the diameter of semicircle in undoped is larger than that in doped PPy system. On the other hand, it can be found that the undoped PPy having higher charge transfer resistance are electrochemically inactive [37], whereas the doped PPy hav-

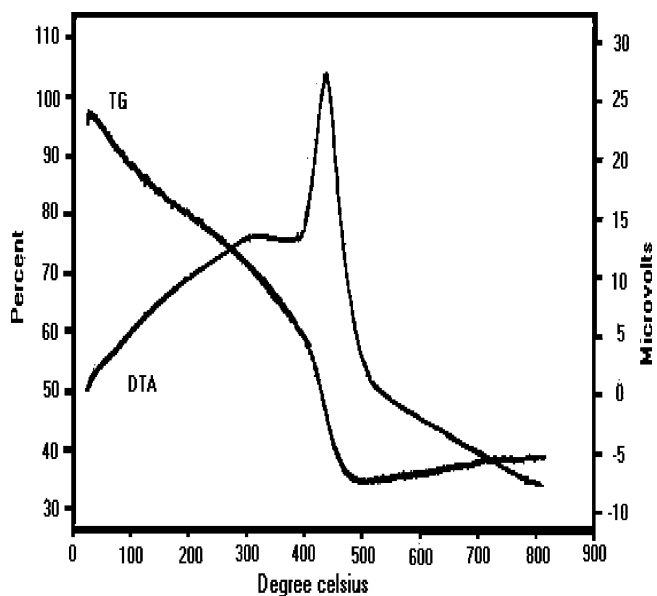


Fig. 9. TG/DTA curve for undoped PPy.

ing a small radius of curvature indicates low resistance to charge transfer process.

Table 1 gives the  $R_s$ ,  $R_{ct}$  and  $C$  values of doped and undoped PPy film synthesized, using room temperature melt.

It was found that the charge transfer resistance ( $R_{ct}$ ) increases to the nine times the greater values for undoped PPy when compared to doped species. From this, it is evident that the reactivity of doped PPy film is very high, and, hence when exposed to air it is easily attacked by moisture and a passive layer is formed which loses conductivity and reactivity, and, thus attains the undoped form. This is evident from the impedance values, which are high in the high frequency region for the undoped form and consequently low conductivity, while that of doped form reaches the origin of the graph stressing that it is highly conducting in nature.

### 3.6. Conductivity measurements

The conductivity of freshly deposited PPy (doped) film is around  $133 \text{ S cm}^{-1}$ . But gradually when exposed to air this conductivity decreases.

This is because, after exposure to air the dopant in doped PPy film reacts with moisture to yield aluminum oxy chloride and aluminum hydroxide, thereby the undoping occurs,

however this PPy film can be redoped. The conductivity of undoped PPy was observed to be in  $10^{-9} \text{ S cm}^{-1}$ . The dc conductivity obtained from the four-probe method is more accurate as it involves direct measurement of resistance of the polymer films, whereas the impedance is the combination of solution resistance and the two resistor–capacitor combination of two electrodes. Hence, it is not justified to compare the two methods to get the dc conductivity of the film.

### 3.7. UV–vis–NIR spectroscopic studies

The diffused reflectance UV–vis–NIR spectra of (a) doped and (b) undoped PPy are shown in Fig. 6.

The absorption peak observed between 350 and 390 nm is assigned to  $\Pi$ – $\Pi^*$  transition associated with benzenoid ring. The band due to cation radicals lie between 400 and 600 nm. The band observed near or more than 800 nm is due to the charge carriers. The tail of this band extends to the infra-red region indicating that the charge carriers are bipolarons or otherwise called as trapped excitons.

The first absorption peak around 0.7 eV (1264 nm) can be related to a transition from the valance band to the half filled polaron bonding level while the peak around 1.4 eV (882 nm) associated with the transition between bonding and

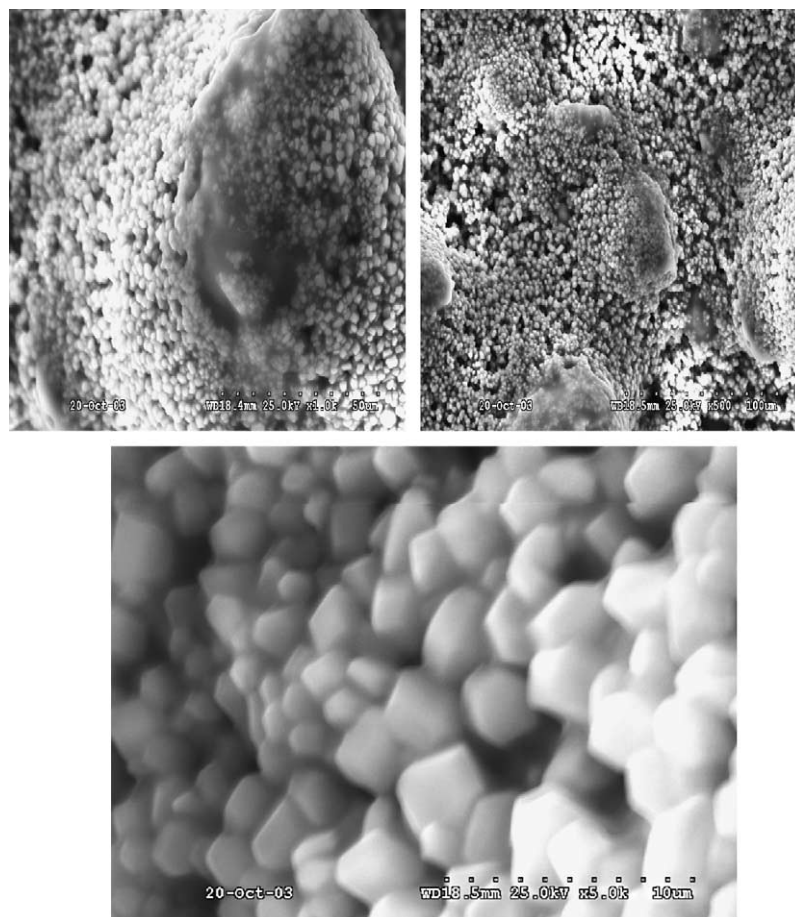


Fig. 10. Scanning electron micrograph of conducting PPy film showing crystalline structure.



antibonding polaron levels. The peak around 2.1 eV (457 nm) corresponds to the transitions from valance band to the antibonding polaron state. As the extent of oxidation increases, bipolaron formation increases. The bipolaron introduces the two states in the gap, at 0.75 eV above the valance band edge and 0.79 eV below the conduction band edge. However, the bonding bipolaron state is empty, the presence of bipolarons leads to only two optical transitions in the gap which explains the appearance of absorption spectra at higher oxidation levels where the two intense bands within the gap are accounted for the two wide bipolaron bands. It is important to note that the gap between these bipolaron bands never goes to zero even at the highest doping levels achieved. Hence, polypyrrole is never a metal.

### 3.8. FTIR spectroscopic studies of PPy film

Principal absorption bands observed in the IR spectra of doped and undoped polypyrrole are given in the Table 2.

All the characteristic IR absorption bands due to polypyrrole are observed in doped PPy film with a slight shift in the position of absorption band. For example, a band at  $3400\text{ cm}^{-1}$  due to NH stretching in neutral PPy vanishes in the doped form and  $1529\text{ cm}^{-1}$  band due to C=C stretching has been observed at  $1545\text{ cm}^{-1}$  in doped film. The spectrum of oxidized form of polypyrrole polymer does not show the NH or CH stretching because there is a strong electronic absorption. Fig. 7 shows the FTIR spectra for PPy films.

### 3.9. Thermal studies

Figs. 8 and 9 shows the thermogravimetric curves of doped and undoped PPy film respectively. In the thermogram of undoped PPy, the DTA curve shows a remarkable peak at  $450^\circ\text{C}$ , indicating the breakdown of polymer backbone. On the other hand, there is a peak at  $440^\circ\text{C}$  in the doped species, which may be due to the expulsion of the dopant and polymer degradation occurs at  $600^\circ\text{C}$ . The TG curve shows no weight loss up to  $400^\circ\text{C}$  and decomposition of the polymer backbone in the undoped species occurs from  $550^\circ\text{C}$ . In the doped polymer it is two-step degradation and the first weight loss ( $-4\%$ ) is observed up to  $100^\circ\text{C}$  possible due to moisture content entrapped in the polymer matrix. From  $400$  to  $500^\circ\text{C}$  the weight loss is corresponding to the weight of the dopant. The residual weight in doped PPy is less than that in undoped showing the less thermal stability. The decrease in thermal stability in this case may be due to the formation of several low molecular weight species during thermo-oxidative degradation.

### 3.10. SEM pictures

Figs. 10 and 11 are the scanning electron micrographs of doped and undoped PPy, respectively. Figure 10 shows that doped polymer has a regular hexagonal geometry. The study shows that the size of the largest hexagon is  $3.5\text{ }\mu\text{m}$  and that

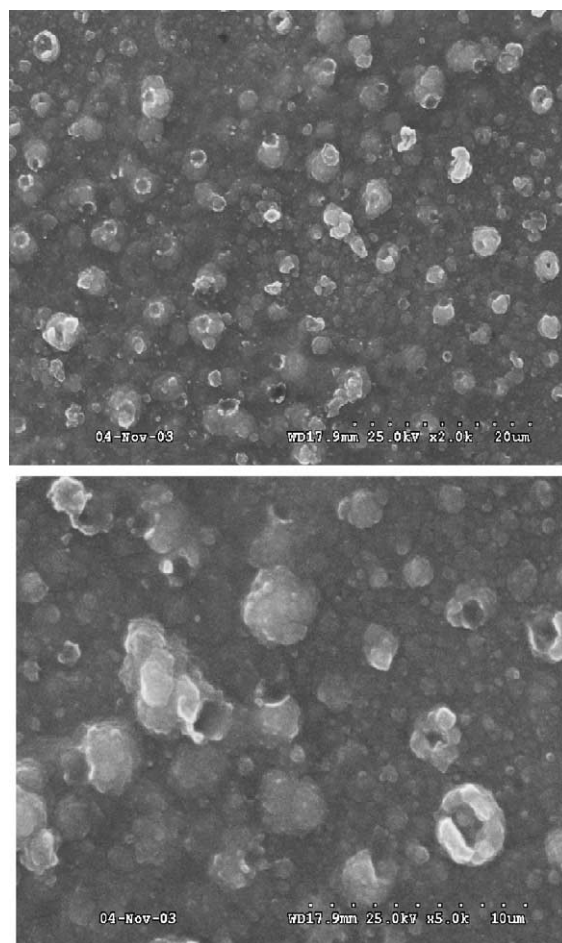


Fig. 11. Scanning electron micrograph of undoped PPy film showing non-conducting dark portions.

of smallest is  $2.5\text{ }\mu\text{m}$  and the undoped polymer has globular structures with particle size ranging from  $0.85$  to  $14.7\text{ }\mu\text{m}$ . The brightness of hexagon in a uniform way indicates the homogeneity of doping.

## 4. Conclusion

Pyrrole can be anodically polymerized at comparatively lower potentials in acidic room temperature melt as an electrolyte to yield a black, highly conducting free standing PPy film. The  $\text{Al}_2\text{Cl}_7^-$  anion generated from the melt has equal bond lengths and bond angles giving rise to a well-ordered polymer.

## References

- [1] G.P. Gardini, Adv. Heterocycl. Chem. 15 (1973) 67.
- [2] A. Dall'olio, Y. Dascola, V. Varacco, V. Bochi, C.R. Acad. Sci. Ser. C. 267 (1968) 433.
- [3] G.B. Street, T.C. Clarke, M. Kroumbi, K.K. Kanazawa, V. Lee, P. Pfluger, J.C. Scott, G. Weiser, Mol. Cryst. Liq. Cryst. 83 (1982) 253.

- [4] M. Salmon, K.K. Kanazawa, A.F. Diaz, N. Krounbi, *J. Polym. Sci. Polym. Lett. Ed.* 20 (1982) 20.
- [5] K.K. Kanazawa, A.F. Diaz, W.D. Gill, P.M. Grant, G.B. Street, G.P. Gardini, J.F. Kwak, *Synth. Met.* 1 (1980) 329.
- [6] K.K. Kanazawa, A.F. Diaz, R.H. Geiss, W.D. Gill, J.F. Kwak, J.A. Logan, J.F. Rabolt, G.B. Street, *J.Chem.Soc. Chem.Commun.* (1979) 854.
- [7] A.F. Diaz, K.K. Kanazawa, G.P. Gardini, *J. Chem. Soc. Chem.Commun.* (1979) 635.
- [8] J.C. Vidal, E. Garcia, J.R. Castillo, *Anal. Chim. Acta.* 385 (1–3) (1999) 213.
- [9] T.E. Campbell, A.J. Hodgson, G.G. Wallace, *Electroanalysis* 11 (4) (1999) 215.
- [10] D. Kincal, A. Kamer, A.D. Child, J.R. Reynold, *Synth. Met.* 92 (1998) 53.
- [11] N.T. Kemp, G.U. Flanagan, A.B. Kaiser, H.J. Trodahl, B. Chapman, A.C. Partridge, R.G. Buckley, *Synth. Met.* 101 (1999) 434.
- [12] C. Jérôme, D. Labaye, I. Bodart, R. Jérôme, *Synth. Met.* 101 (1999) 3.
- [13] E. Smela, *J. Micromech. Microeng.* 9 (1) (1999) 1.
- [14] S.C. Yang, H. Liu, R.L. Clark, *PCT Int. Appl. WO 9922,380 (Cl.H01 B1/00)*.
- [15] T. Takamatsu, Y. Taketani, *Jpn. Kokai. Tokyo Koho JP11121, 279 (99121, 279)*.
- [16] Y. Kojima, H. Kamikawa, T. Takamatsu, *Jpn. Kokai. Tokyo Koho JP11121, 280 (99121, 280)*.
- [17] T.A. Skotheim (Ed.), *Handbook of Conducting Polymers*, vols. I and II, Marcel Dekker, New York, 1986.
- [18] *Handbook of Conducting Polymers*, Marcel Dekker, New York, 1998.
- [19] G.G. Wallace, G. Spinks, P.R. Teasdale, *Conductive Electroactive Polymers*, Technomic, New York, 1997.
- [20] J.O. Iroh, C. Williams, *Synth. Met.* 99 (1999) 1.
- [21] W. Su, J.O. Iroh, *Synth. Met.* 95 (1998) 159.
- [22] J.R. Reynolds, L. Hiep, F. Selampinar, P.J. Kinlen, *Polym. Prepr (Am. Chem. Soc., Div. Polym.Chem.)* 40 (1) (1999) 307.
- [23] W.K. Lu, R.A. Elsenbaumer, *Annu. Tech. Conf. Soc. Plast. Eng.* 56 (2) (1998) 1276.
- [24] K. Fraoua, S. Aeiyaich, J. Aubard, M. Delamar, P.C. Lacaze, C.A. Ferreira, *J. Adhes. Sci. Technol.* 13 (4) (1999) 517.
- [25] T. Ito, P. Buehlmann, Y. Umezawa, *Anal. Chem.* 71 (9) (1999) 1699.
- [26] Dinesh Chandra Trivedi, *J.Chem. Soc., Chem. Commun.* (1989) 544.
- [27] A.A. Fannin, A.A. Floreani, D.A. King, L.A. Landers, J.S. Piersma, B.J. Stech, B.J. Vaughn, R.L. Wikes, J.S. Williams, *J. Phy. Chem.* 88 (1984) 2614.
- [28] F.M. Fowkes (Ed.), *Physicochemical Aspects of Polymer Surfaces.*, vol. 2, Plenum Press, New York, 1983, p. 583.
- [29] A.F. Diaz, K.K. Kanazawa, *Chem. Scr.* 17 (1981) 145.
- [30] E.M. Genies, G. Bidan, A.F. Diaz, *J. Electroanal. Chem.* 149 (1983) 101.
- [31] T.A. Witten, L.M. Sanders, *Phys. Rev. Lett.* 47 (1981) 1400.
- [32] P. Meakin, *Phy. Rev. A* 33 (1986) 1984.
- [33] F. Li, W.J. Albery, *Electrochim. Acta* 37 (1992) 393.
- [34] L. Niu, Q. Li, F. Wei, X. Chen, H. Wang, *J. Electroanal. Chem* 544 (2003) 121.
- [35] K. Juttner, *Electrochim. Acta* 35 (1990) 1501.
- [36] Pajkossy, *J. Electroanal. Chem* 364 (1994) 111.
- [37] P. Ferloni, M. Mastragistino, L. Meneghello, *Electrochim. Acta* 41 (1) (1996) 27.